JOURNAL OF MATERIALS SCIENCE 24 (1989) 4392–4398

A.c. conduction mechanism and dielectric properties of co-evaporated SiO/B_2O_3 amorphous thin films

M. H. ISLAM, C. A. HOGARTH
Department of Physics, Brunel University, Uxbridge, Middlesex UB8 3PH, UK

The a.c. electrical properties on Al–SiO/B_2O_3–Al sandwich devices with various compositions of SiO/B_2O_3 were studied over a frequency range of 2×10^2 to 1×10^6 Hz and in the temperature range 158 to 463 K. The a.c. conductance G varies with frequency according to the relation $G \propto \omega^s$, where the exponent s was found to be 0.92 (at 158 K) in the frequency range 8×10^2 to 2×10^4 Hz and above 10^5 Hz the conductance shows a square law dependence on frequency. These results suggest that the a.c. conduction mechanism in SiO/B_2O_3 thin films is due to an electronic hopping process. The numbers of localized sites were calculated using the conductivity relations given by Elliott and by Pollak and the results are compared. The effects of composition, temperature and annealing on the dielectric constant and loss factor were studied. The relative dielectric constant and loss factor were found to decrease with the increase of B_2O_3 content in SiO. Annealing of the samples reduces the values of the dielectric constant, loss factor tan δ, temperature coefficient of capacitance and a.c. conductivity. The variation in capacitance with the composition of SiO/B_2O_3 was investigated at room temperature, the results being normalized to 10 kHz. The dispersion was found to decrease with the addition of B_2O_3 into SiO.

1. Introduction

In recent years considerable interest has been developed in the study of dielectric properties of thin films due to their importance in electronic and optical devices. Evaporated SiO thin films are widely used as a capacitor dielectric in integrated circuits [1]. The addition of B_2O_3 to SiO reduces the dielectric loss in the composite films and thus the films are more suitable for dielectric applications [2, 3]. Timson and Hogarth [4] reported that the co-evaporated SiO/B_2O_3 films have a higher resistivity than SiO films prepared under similar conditions. They attributed this increase of resistivity to the reduced spin density and hence to the density of unpaired electrons when B_2O_3 is added to SiO. Vardhan *et al.* [3] have studied the dielectric properties of SiO/B_2O_3 prepared from a single source and reported that a minimum of dielectric loss occurs at 5% B_2O_3 in the mixture. The d.c. electrical properties of metal–SiO/B_2O_3–metal sandwiches have been thoroughly investigated by a number of authors [5–8]. A limited study of the a.c. electrical conductivity of SiO/B_2O_3 has been reported by Timson and Hogarth [4] in the frequency range 100 Hz to 20 kHz.

It is of interest to make a further study of the a.c. electrical properties of co-evaporated SiO/B_2O_3 thin films because of the good dielectric characteristics. In this paper the a.c. electrical conductivity and dielectric properties of Al–SiO/B_2O_3–Al sandwich devices are reported over the frequency range 2×10^2 Hz to 1 MHz. The effects of annealing and temperature of operation on the dielectric properties are also reported.

2. Experimental work

Thin films of SiO/B_2O_3 were prepared using the co-evaporation technique developed by Hogarth and Wright [6] in a Balzers Ba510 coating unit at a pressure of about 3×10^{-4} Pa and deposited onto clean 7059 Corning glass substrates. The substrate temperature was kept at 373 K during the evaporation of the materials to improve the adhesion of the films. Tantalum and molybdenum boats were used for SiO and B_2O_3 respectively and a tungsten spiral was used for the evaporation of aluminium. Six devices with an active area of 0.08 cm^2 were prepared on each substrate. The deposition rates of SiO and B_2O_3 were 1.5 and 1.0 nm sec^{-1} respectively. The insulator thickness was 290 mm for all compositions. Two quartz crystal monitors were used to monitor the thickness of the films and the rate of evaporation. The thickness of the films was measured finally by using an optical interferometric method. The a.c. conductance, capacitance and loss factor were measured directly with the help of a Hewlett-Packard impedance analyser (5 Hz–13 MHz), type 4192 A LF. An a.c. signal of 500 V_{rms} was applied across the sample. The measurements were made before and after annealing of the device over the temperature range 158 to 463 K. Some samples were annealed in a vacuum of about

0022–2461/89 $03.00 + .12

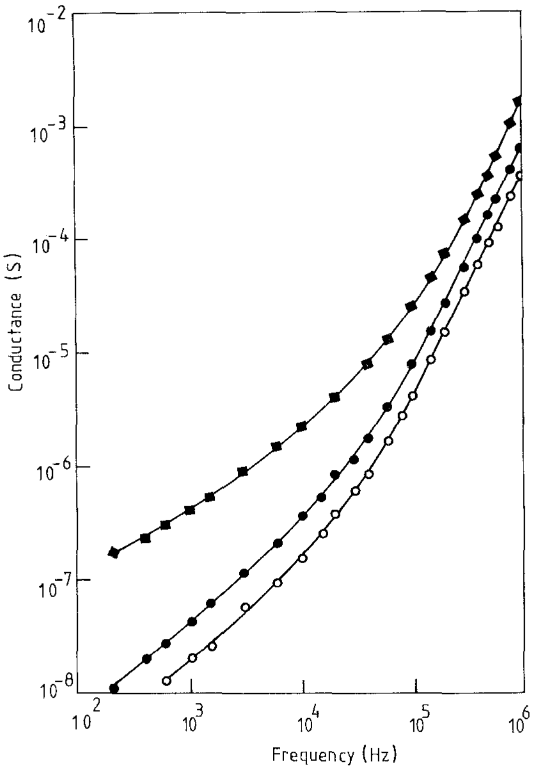

Figure 1 The variation of a.c conductance with frequency for films of SiO and SiO/B_2O_3. (■) 100% SiO; (●) 85% SiO/15% B_2O_3; (○) 70% SiO/30% B_2O_3.

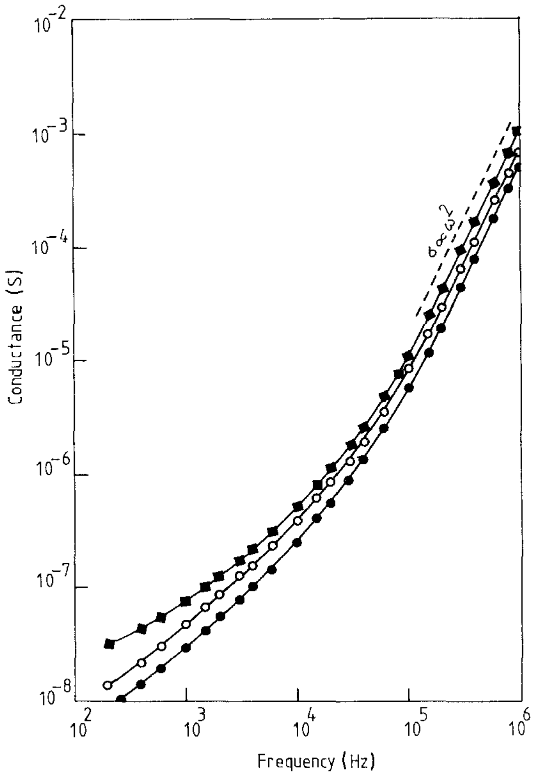

Figure 2 Frequency dependence of the conductance of an Al–85% SiO/15% B_2O_3–Al (insulator thickness 190 nm) device at different temperatures. (■) 463 K; (○) 345 K; (●) 158 K.

10^{-3} Pa at 473 K for 2 h. Sample temperatures were measured using a copper/constantan thermocouple connected to the sample.

3. Results

3.1. A.c. electrical conductivity

The total a.c. conductance (G) was measured in the frequency range 2×10^2 to 10^6 Hz. The variation of G with frequency at room temperature for SiO and for composite films of SiO/B_2O_3 is shown in Fig. 1. The frequency dependence of a.c. conductance is of the form

$$G(\omega) = A\omega^s \qquad (1)$$

where A and s are parameters and ω is the angular frequency of measurement. The parameter s may itself be a weak function of temperature and frequency. It is observed from Fig. 1 that the conductance decreases with the increase of B_2O_3 content in the film. The slopes of the log G against log f graphs were calculated and are recorded in Table I (f is frequency = $\omega/2\pi$). It is found that the slope s increases with the addition of B_2O_3 into SiO but does not show any significant difference with the increasing percentage of B_2O_3 into the matrix. For composite films the index s lies between 0.88 and 1 in the frequency range 8×10^2–3×10^4 Hz and the result is in good agreement with the earlier results of Timson and Hogarth [4]. Above 10^5 Hz the conductance increases more strongly with frequency and follows an ω^2 law. Figure 2 shows the plots of log G against log f at different temperatures for an Al–85 mol % SiO/15 mol % B_2O_3–Al device. The slope s was found to be independent of temperature above 10^4 Hz and weakly temperature-dependent (decreasing with increase of temperature) below 10^4 Hz.

A plot of log σ against $1/T$ at five fixed frequencies is shown in Fig. 3 for the same sample shown in Fig. 2 and shows that the conductivity (σ) is weakly temperature-dependent at low temperature and becomes much less dependent at higher temperatures. The activation energies were calculated at each fixed frequency for different temperature ranges and are also given in Table II. It is evident from this table that the activation energy is frequency-dependent and that it decreases with increase of frequency. This is in agreement with the earlier results [4]. The activation energy increases with increase of temperature but still keeps a low value in the range 68 to 32 meV (the lower value for the higher frequency) in the high-temperature region (400–460 K).

TABLE I The values of the index s at room temperature for SiO and SiO/B_2O_3 thin films

Composition	Values of the parameter s at room temperature and in three frequency ranges		
	8×10^2–2×10^3 Hz	2×10^3–1×10^4 Hz	10^5–10^6 Hz
100% SiO	0.70	0.75	1.7
85 mol % SiO/15 mol % B_2O_3	0.88	0.92	2.0
70 mol % SiO/30 mol % B_2O_3	0.86	0.90	2.0

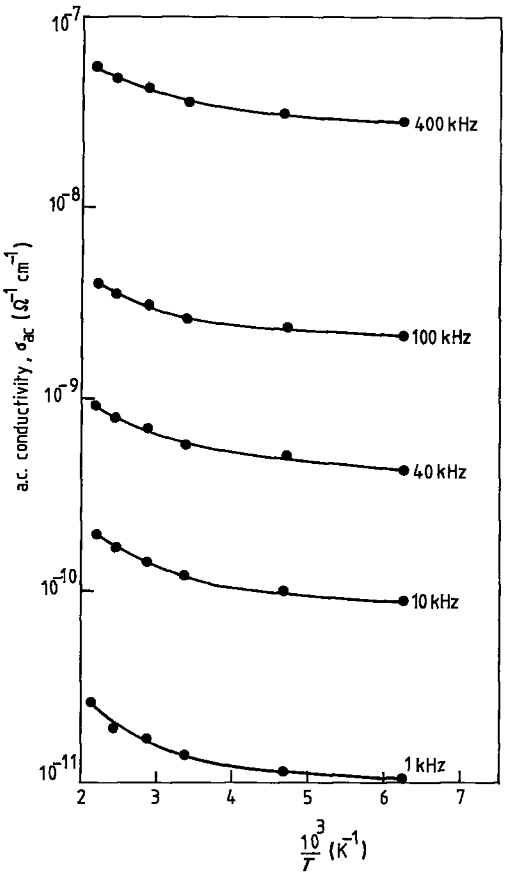

Figure 3 Semilog plots of the a.c. conductivity (σ_{ac}) as a function of reciprocal temperature for the same film as in Fig. 2, at various frequencies.

3.2. Dielectric properties

3.2.1. Effect of composition and frequency

The variation of capacitance with frequency at room temperature for SiO and for two different compositions of SiO/B_2O_3 is shown in Fig. 4. The capacitance is found to decrease with the addition of B_2O_3 into SiO and it is almost constant in the entire frequency range studied for the SiO/B_2O_3 composite films.

The relative variation in capacitance $\Delta C/C$ with frequency at room temperature and normalized at 10 kHz is shown in Fig. 5 for SiO and for two different compositions of SiO/B_2O_3. It is clear from this figure that the relative capacitance decreased drastically with the addition of B_2O_3 into the SiO. The real part of the dielectric constant ε_r' was calculated using the relation

TABLE II The values of the activation energy ΔE(eV) at various fixed frequencies and in three temperature ranges

Frequency (kHz)	Activation energy ΔE (eV) for different temperature ranges		
	400–460 K	286–400 K	158–213 K
1	0.068	0.041	0.0064
10	0.047	0.032	0.0058
40	0.040	0.033	0.0038
100	0.033	0.029	0.0036
400	0.032	0.026	0.0036

$$C = \varepsilon_0 \varepsilon_r' A/d \qquad (2)$$

where ε_0 is the dielectric constant of free space, A is the device active area and d is the sample thickness. Figure 6 shows the plot of dielectric constant ε_r' against frequency for the same film as shown in Fig. 4. It may be seen from Fig. 6 that the dielectric constant decreases with the increase of B_2O_3 content in the SiO. The dielectric constant changes by only 3% for 85% SiO/15% B_2O_3 samples in the frequency range 2×10^2 to 1×10^6 Hz, whereas the dispersion is 12% for SiO in the same frequency range.

The variation of loss factor (tan δ) with frequency for different compositions of SiO/B_2O_3 is shown in Fig. 7. It is found that the loss factor decreases with the increase of B_2O_3 content into SiO and a minimum in tan δ is observed for all compositions as has previously been observed in many insulating thin films [9–12].

3.2.2. Effect of temperature and annealing

Figure 8 shows the typical variation of capacitance with temperature at five different fixed frequencies for an Al–85% SiO/15% B_2O_3–Al sandwich device (insulator thickness ~290 nm). It is found that the capacitance increases with temperature for all frequencies and after attaining a maximum value at 342 K, the capacitance decreases with further increase of temperature.

The variation of the real part of dielectric constant ε_r' with temperature at various fixed frequencies is

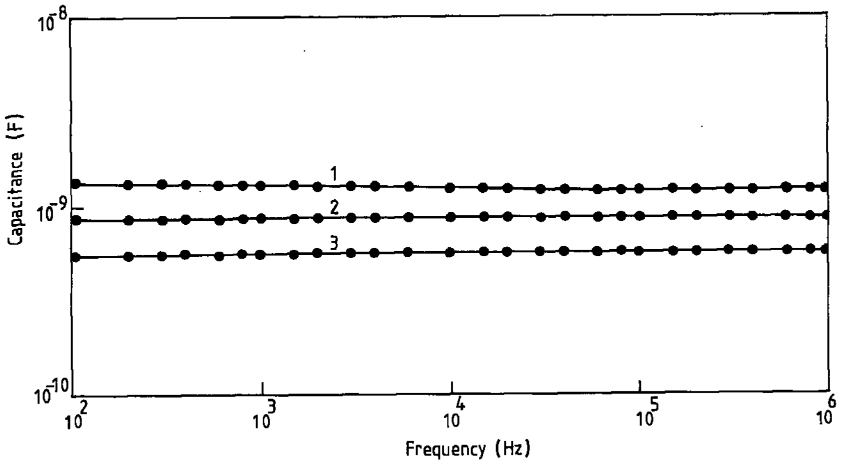

Figure 4 The variation of capacitance with frequency for SiO and two different compositions of SiO/B_2O_3. (1) 100% SiO; (2) 85% SiO/15% B_2O_3; 70% SiO/30% B_2O_3.

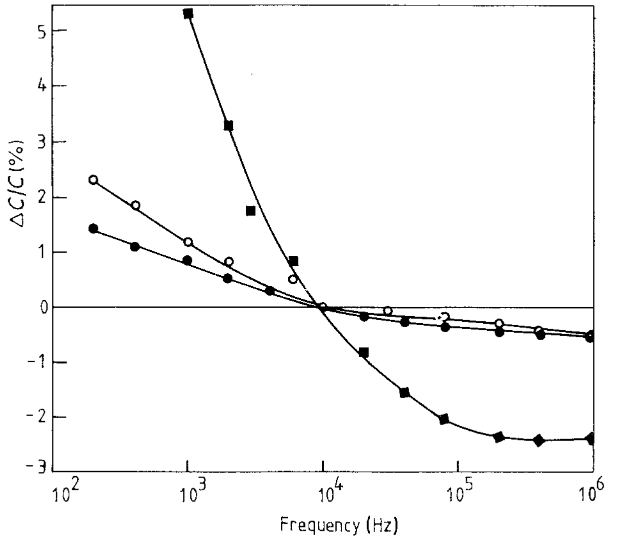

Figure 5 Plots of $\Delta C/C$ (%) as a function of frequency at room temperature for SiO. (■) 100%; (○) 85% SiO/15% B_2O_3; (●) 70% SiO/30% B_2O_3.

shown in Fig. 9. As the dielectric constant is directly proportional to capacitance, for fixed film thickness, the variation of dielectric constant with temperature is the same as in Fig. 8.

The capacitance measurements at different temperatures were performed before and after annealing of the device. Figure 10 shows the effect of heating and cooling cycles on the variation of capacitance with temperature at 100 kHz for the same film as in Fig. 8. It is observed that the capacitance peak obtained in the first temperature cycle (before annealing) disappears in the second cycle of heating and cooling. It is also seen that the value of capacitance decreases considerably after annealing of the film during the first heating cycle.

Figure 11 shows the typical variation of tan δ with temperature at five fixed frequencies for the same film in Fig. 8. It may be seen that the value of tan δ increases with temperature and that the variation is less in the low temperature region.

The variations of capacitance and tan δ with frequency at room temperature (before and after annealing) are shown in Fig. 12 for 85 mol % SiO/15 mol % B_2O_3. It is found that both capacitance and tan δ decrease after annealing of the film.

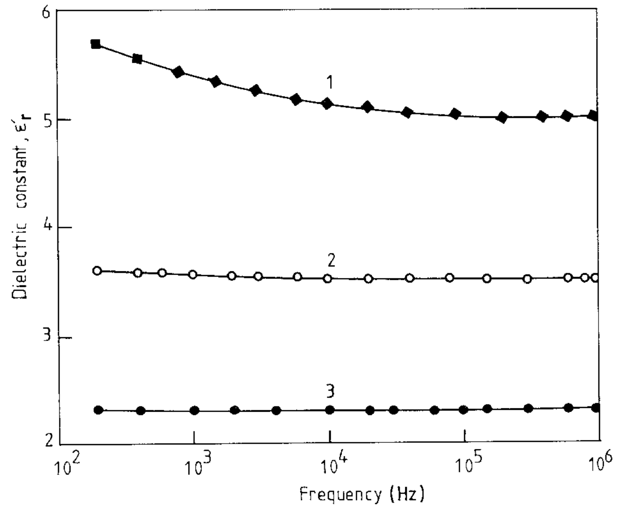

Figure 6 Variation of dielectric constant with frequency at room temperature for films of (1) 100% SiO, (2) 85% SiO/15% B_2O_3; (3) 70% SiO/30% B_2O_3.

TABLE III The effect of annealing on the dielectric properties of 85 mol % SiO/15 mol % B_2O_3 thin film capacitors measured at 10 kHz

Property	Before annealing	After annealing	Variation
Relative dielectric constant (ε_r')	3.51	3.41	−2.9%
Dielectric loss (tan δ)	0.0064	0.0040	−37.5%
TCC (K^{-1})	9.53×10^{-5}	8.58×10^{-5}	−9.97%
Electrical conductivity σ ($\Omega^{-1}\,cm^{-1}$)	1.20×10^{-10}	7.37×10^{-11}	−39.6%

The temperature coefficient of capacitance (TCC) before and after annealing was calculated using the relation

$$\mathrm{TCC} = 1/C_{293\,\mathrm{K}}\, \mathrm{d}C/\mathrm{d}T \qquad (3)$$

and the results are given in Table III.

The effect of annealing on the dielectric properties of an Al–85 mol % SiO/15 mol % B_2O_3–Al thin film capacitor at 10 kHz are summarized in Table III.

It may be seen from Table III that the dielectric loss changes by −37.5% to the low value of tan δ = 0.004 at a frequency of 10 kHz. During the heat treatment the TCC decreases by 10% to the low value of $8.58 \times 10^{-5}\,K^{-1}$ in the temperature range 293 to 343 K. The dielectric constant decreases by only 2.85% and the a.c. conductivity decreases by 39.6% during the annealing process of the device. To see the ageing effect on the capacitance, the film was kept in a vacuum over a period of 8 months. The capacitance decreased by only 3.8% in 8 months of ageing time.

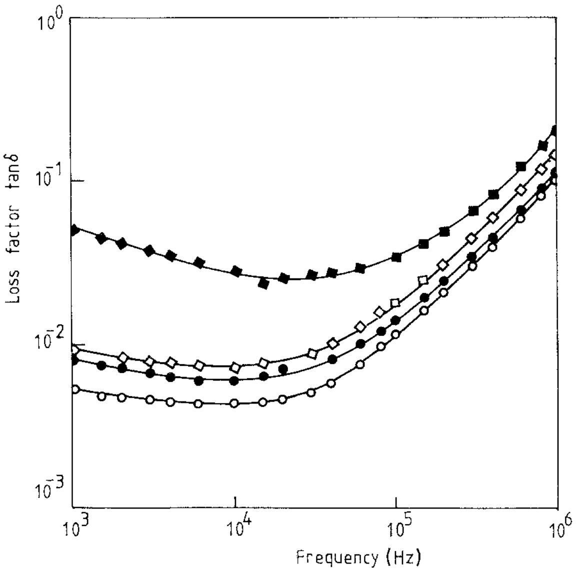

Figure 7 The variation of loss factor tan δ as a function of frequency at room temperature for SiO and SiO/B_2O_3 thin films: (◆) 100% SiO; (◇) 88% SiO/12% B_2O_3; (●) 85% SiO/15% B_2O_3; (○) 70% SiO/30% B_2O_3.

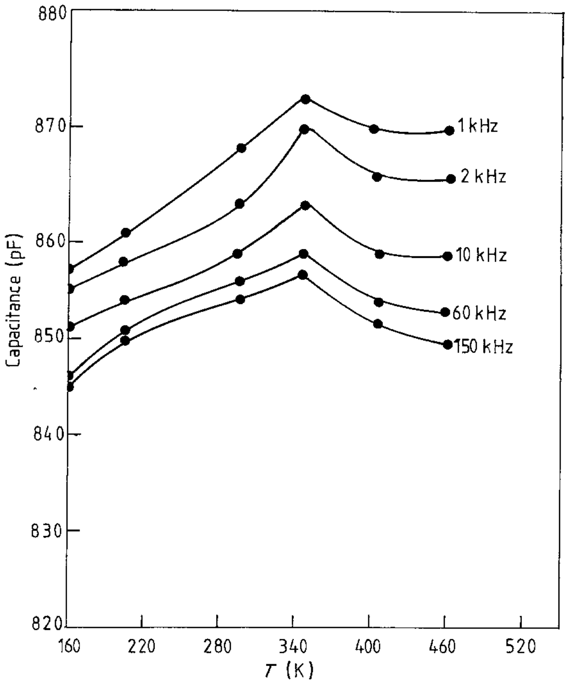

Figure 8 Variation of capacitance with temperature of 85% SiO/15% B_2O_3, at various frequencies.

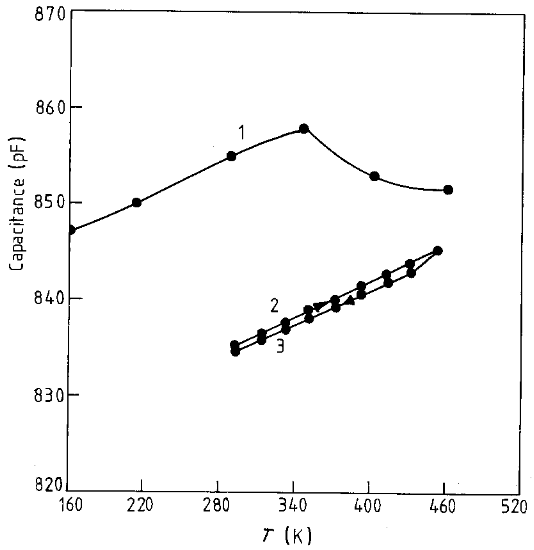

Figure 10 Variation of capacitance with temperature at 100 kHz of an Al–85% SiO/15% B_2O_3–Al device for different heating and cooling cycles: (1) 1st heating cycle; (2) 2nd heating; (3) 2nd cooling.

4. Discussion

The variation of a.c. conductance with frequency was found to obey the relation $G \propto \omega^s$ for a given frequency range (below 10^4 Hz) and independent of temperature at the higher frequencies (above 10^4 Hz). At low temperature (158 K) the value of s for 85 mol % SiO/15 mol % B_2O_3 is found to be 0.92 in the frequency range 8×10^2 to 2×10^4 Hz and it increases to ~ 2 at frequencies above 10^5 Hz. The measured activation energy in the low temperature region (158–213 K) lies between 3.6 and 6.4 meV (lower values for higher frequencies) in the frequency range 1×10^3 to 4×10^5 Hz. The strong frequency dependence of conductivity at high frequencies (Fig. 2), a low activation energy at low temperatures (Table II) and an absence of dispersion of permittivity at high frequencies (Fig. 6), are all features which suggest that the conduction mechanism is based on electronic hopping [13]. The low values of the activation energies (0.032 to 0.68 eV) in the high temperature region (400 to 460 K) are an indication that hopping conduction is still predominant at the higher temperatures.

The square law dependence of conductivity on frequency may be a continuation of the low frequency process [14]. As the frequency increases the hops will become shorter and in the limit of interatomic distances, will no longer be randomly distributed leading naturally therefore to a frequency dependence which tends to ω^2. Such an effect has also been reported by other authors for various oxide thin films and glasses [14–16].

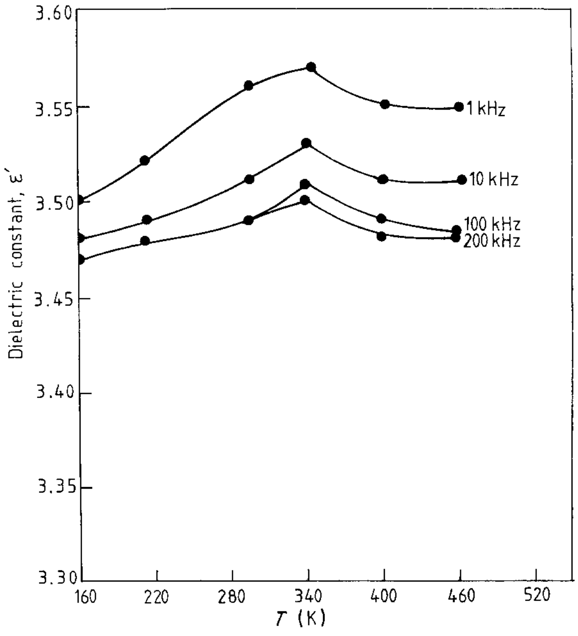

Figure 9 Variation of dielectric constant with temperatures at different frequencies for the same film as in Fig. 8.

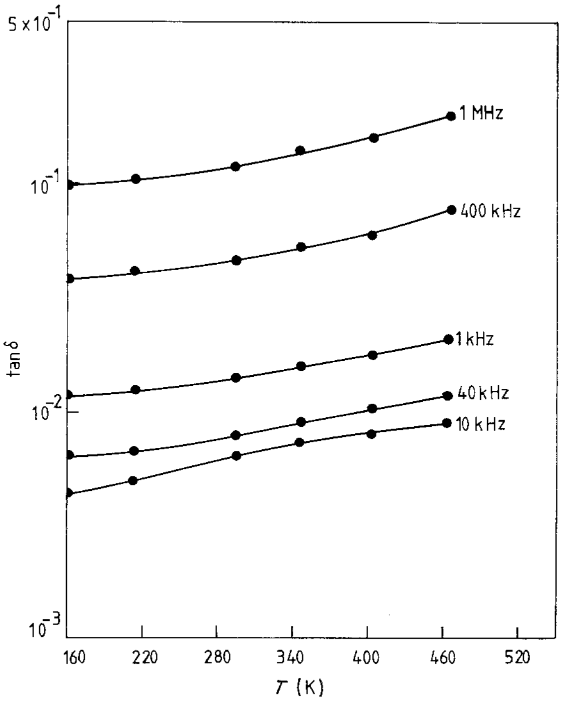

Figure 11 Variation of loss factor tan δ with temperature at various frequencies for the same film as in Fig. 10.

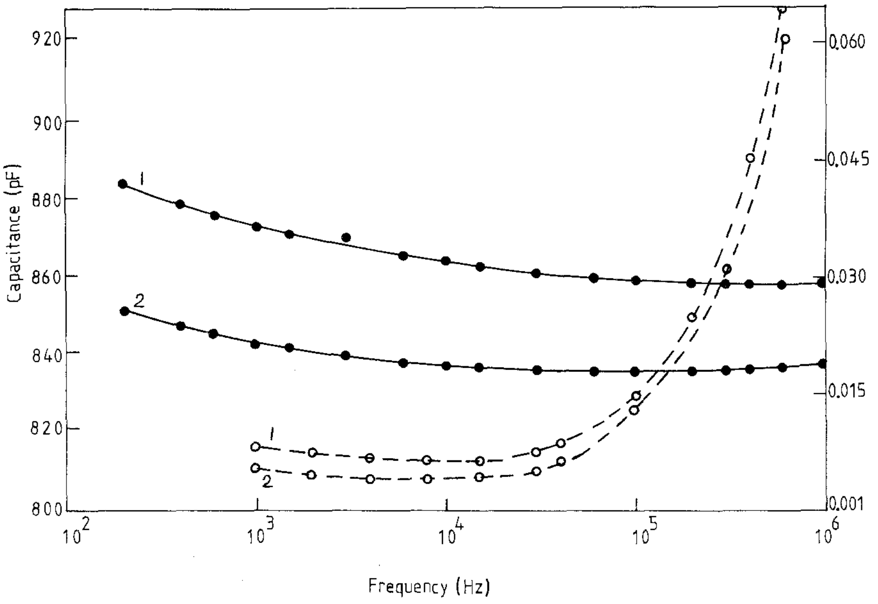

Figure 12 Variation of capacitance (——) and tan δ (- - -) with frequency (before and after annealing) for an Al–85% SiO/15% B_2O_3–Al device. (1) Before annealing; (2) after annealing.

Elliott [17] proposed a model for a.c. conduction in chalcogenide glasses which has been used to explain the frequency and temperature dependent conductivity of many amorphous thin films and glasses [18–20]. The Elliott model seems to be appropriate to explain the a.c. conductivity data for these quasi-glassy SiO/B_2O_3 films. The expression for a.c. conductivity $\sigma(\omega)$ derived by Pollak [21] is as follows

$$\sigma(\omega) = \pi^3/96e^2kT[N(E_F)]^2a^5\omega[\ln(1/\omega\tau_0)]^4 \quad (4)$$

where $N(E_F)$ is the density of states at the Fermi level ($cm^{-3}\,eV^{-1}$), a is the radius of the localized wave function and τ is a relaxation time.

Equation 4 cannot explain the experimentally observed temperature dependence of the exponent s of the frequency dependence of conductivity, nor the variation of activation energy with frequency [18]. However, Equation 1 for a.c. conductivity given by Elliott [18] satisfactorily explains the variation of activation energy with frequency as observed experimentally in this study. The value of $N(\approx 10^{17}\,cm^{-3})$ obtained from a.c. measurements in this study is comparable with the value of spin density obtained from electron-spin resonance measurements [6, 22].

It is found that the capacitance and hence the dielectric constant decrease with the addition of B_2O_3 into SiO (Figs 4 and 6). This decrease of capacitance and dielectric constant with composition of SiO/B_2O_3 may be explained in the following manner. Timson and Hogarth [5] and Dubey *et al.* [22] suggested that with the addition of B_2O_3 into SiO a considerable reduction occurs in the number of dangling bonds within the material. Because of the reduced dangling bond density and of the associated reduction in the density of charge carriers, less polarization occurs in SiO/B_2O_3 relative to SiO under the same applied a.c. electric field, resulting in a decrease of capacitance and hence of the dielectric constant. The present results are contradictory with the results reported by Vardhan *et al.* [3] for SiO/B_2O_3 prepared from a single source. They reported that the dielectric constant increases with the addition of B_2O_3 into SiO.

The reduction of dielectric loss with the addition of B_2O_3 into SiO may be due to the reduction of the number of weak percolation paths through the insulator when B_2O_3 is added to the SiO. During evaporation of B_2O_3 and SiO an enhanced oxygen adsorption occurs [5] and this may lead to improved dielectric properties.

The capacitance increases with increasing temperature (Fig. 8) because of the increase in the mobility of the charge carriers at higher temperatures but after attaining a maximum value the capacitance decreases with further increase of temperature. This may arise for the following reasons. According to Morley and Campbell [23] and Chandra Shekar and Hari Babu [24] the dielectric films adsorb gases from the residual atmosphere during film formation. It is also mentioned that SiO/B_2O_3 films absorb water vapour when exposed to the atmosphere [5]. In the subsequent heating and cooling cycles the capacitance peak disappears due to the removal of absorbed moisture and gases in the first heating cycle as shown in Fig. 10. The decrease of capacitance in the second heating cycle (Fig. 10) may be due to the annealing of some defects in the first heating cycle.

The decrease of capacitance and loss factor tan δ (Fig. 12) after annealing of the device, may be associated with the removal of some voids and dangling bonds and rearrangement of some atoms during the annealing process. Similar results were also found by Goswami and Varma [10] for dysprosium oxide films.

References

1. G. SIDDALL, "Thin film microelectronics", edited by L. Holland (Chapman and Hall, London, 1965) Vol. 1.
2. W. HANLEIN and K. G. GUNTHER, "Advances in vacuum science and technology" (Pergamon, Oxford, 1960).
3. H. VARDHAN, G. C. DUBEY and R. A. SINGH, *Thin Solid Films* **8** (1971) 51.

4. P. A. TIMSON and C. A. HOGARTH, *ibid.* **10** (1972) 321.
5. *Idem, ibid.* **8** (1971) 237.
6. C. A. HOGARTH and L. A. WRIGHT, Proceedings of the 9th International Conference on the Physics of Semiconductors, Moscow, July 1968 (Acadamy of Science USSR, 1968) Vol. II, p. 1274.
7. C. A. HOGARTH and A. KOMPANY, *Int. J. Electronics* **53** (1982) 301.
8. C. A. HOGARTH and E. H. Z. TAHERI, *ibid.* **37** (1974) 145.
9. C. A. DUTTA and K. BARUA, *Thin Solid Films* **100** (1983) 149.
10. A. GOSWAMI and R. R. VARMA, *ibid.* **28** (1975) 157.
11. A. GOSWAMI and A. P. GOSWAMI, *ibid.* **16** (1973) 175.
12. A. E. HILL, A. M. PHALLE and J. H. CALDERWOOD, *ibid.* **5** (1970) 287.
13. R. M. HILL and A. K. JONSCHER, *J. Non-cryst. Solids* **32** (1979) 53.
14. A. E. OWEN and J. M. ROBERTSON, *ibid.* **2** (1970) 40.
15. W. S. CHAN and A. K. JONSCHER, *Phys. Status Solidi* **32** (1969) 749.
16. F. ARGALL and A. K. JONSCHER, *Thin Solid Films* **2** (1969) 185.
17. S. R. ELLIOTT, *Phil. Mag.* **B36** (1977) 1291.
18. *Idem, ibid.* **B37** (1978) 553.
19. M. MEAUDRE and R. MEAUDRE, *ibid.* **B40** (1979) 401.
20. A. S. M. S. RAHMAN, M. H. ISLAM and C. A. HOGARTH, *Int. J. Electronics* **62** (1987) 167.
21. M. POLLAK, *Phil. Mag.* **23** (1971) 519.
22. G. C. DUBEY, K. SAHU and T. Rs. REDDY, *Thin Solid Films* **61** (1979) L17.
23. A. R. MORLEY and D. S. CAMPBELL, *ibid.* **2** (1968) 403.
24. M. CHANDRA SHEKAR and V. HARI BABU, *J. Mater. Sci. Lett.* **3** (1984) 600.

Received 27 July 1988
and accepted 5 January 1989